Determination of the Rate-Limiting Segment of Aminoglycoside Nucleotidyltransferase 2″-I by pH- and Viscosity-Dependent Kinetics†

Cynthia A. Gates‡ and Dexter B. Northrop*

Division of Pharmaceutical Biochemistry, School of Pharmacy, University of Wisconsin, Madison, Wisconsin 53706

Received August 13, 1987; Revised Manuscript Received January 15, 1988

ABSTRACT: Aminoglycoside nucleotidyltransferase 2″-I follows a Theorell–Chance kinetic mechanism in which turnover is controlled by the rate-limiting release of the final product (Q), a nucleotidylated aminoglycoside [Gates, C. A., & Northrop, D. B. (1988) *Biochemistry* (second of three papers in this issue)]. The effects of viscosity on the kinetic constants of netilmicin, gentamicin C_1, and sisomicin aminoglycoside substrates are as follows: no change in the substrate inhibition constants of all three antibiotics, a small but significant and highly unusual increase in V_{max}/K_m for netilmicin but large, normal decreases for gentamicin C_1 and sisomicin, and marked decreases in the maximal velocities for all three. The lack of effect on substrate inhibition provides essential control experiments, signifying that glycerol does not interfere with binding of aminoglycosides to EQ and that the steady-state distribution of EQ does not increase as the release of Q is slowed by a viscosogen. The decrease in the V_{max}/K_m of better substrates indicates dominance by a diffusion-controlled component in the catalytic segment, attributed to the release of pyrophosphate. The presence of an increase in the V_{max}/K_m of the poor substrate, however, is inexplicable in terms of either single or multiple diffusion-controlled steps. Instead, it is here attributed to an equilibrium between conformers of the enzyme–nucleotide complex in which glycerol favors the conformation necessary for binding of aminoglycosides. The decrease in V_{max} is consistent with the diffusion-controlled release of the final product determining enzymatic turnover. The substrate inhibition constant of sisomicin as a function of pH is a bell-shaped curve with asymptotes of slopes +2 and −2, representing two acidic and two alkaline ionizations, with pK values of 6.68 ± 0.08 and 8.22 ± 0.06, respectively. The pH profile of V_{max}/K_m is strikingly similar, with pK values of 6.76 ± 0.07 and 8.45 ± 0.05. This similarity signifies a common origin and indicates that the aminoglycoside substrate (B) binds to EA in identical fashion as to EQ and that catalysis is pH-independent. Binding identity requires that the aminoglycoside portion of Q does not occupy its subsite on the enzyme; rather, the aminoglycoside portion is released during catalysis, driven by the exothermic loss of a phosphate anhydride bond and stereochemical inversion of the γ-phosphate [Van Pelt, J. E., Iyengar, R., & Frey, P. A. (1986) *J. Biol. Chem. 261*, 15995–15999]. The maximal velocity as a function of pH is described by a shallow wave with a pK of 8.4 ± 0.1. The pH-independent region of the K_i profile coincident with the pH-dependent region of the V_{max} profile shows that the steady-state concentration of EQ is insensitive to changes in pH that affect turnover; thus the kinetic mechanism of the enzyme does not change with pH. The drastic dissimilarity between the pH profiles of V_{max}/K_m and V_{max} confirms the Theorell–Chance kinetic mechanism because these two kinetic constants cannot hold any reactive steps in common.

Alternative substrate and inhibition kinetics on aminoglycoside nucleotidyltransferase 2″-I [ANT(2″)-I] (EC 2.7.7.46) are consistent with a Theorell–Chance kinetic mechanism in which turnover is controlled by the rate-limiting release of the nucleotidylated aminoglycoside product (Gates & Northrop, 1988b). Partial uncompetitive substrate inhibition by aminoglycosides requires that the release of the aminoglycoside precedes the nucleotide moiety of the second product to give an ordered series of steps of product release that are consistent with the reverse of the ordered addition of substrates. Adding conformational changes as a probable origin of ordered binding generates the proposed reaction sequence shown in Scheme I, where A, B, P, and Q represent Mg–ATP, aminoglycoside, Mg–pyrophosphate, and AMP–aminoglycoside, respectively; E_f represents free enzyme in the conformation which binds nucleotides and E_c represents the catalytic conformation of enzyme, the form that binds aminoglycosides; E_fQ represents an enzyme–AMP–aminoglycoside complex with both the nucleotide and aminoglycoside sites occupied and E_f–Q represents an enzyme–AMP–aminoglycoside complex with only the nucleotide site occupied, meaning that the aminoglycoside moiety has been released from the enzyme. The upper sequence of steps is the catalytic segment of the reaction, ending in the irreversible release of Mg–pyrophosphate; the lower sequence is the product-release segment, ending in the release of AMP–aminoglycoside. The proposed rate-limiting segment for enzymatic turnover in a Theorell–Chance mechanism is the latter.[1]

Scheme I

$$E_f \underset{k_2}{\overset{k_1A}{\rightleftharpoons}} E_fA \underset{k_4}{\overset{k_3}{\rightleftharpoons}} E_cA \underset{k_6}{\overset{k_5B}{\rightleftharpoons}} E_cAB \underset{k_8}{\overset{k_7}{\rightleftharpoons}} E_cPQ \xrightarrow{k_9} E_cQ + P$$

$$E_cQ \underset{k_{12}}{\overset{k_{11}}{\rightleftharpoons}} E_c\text{–}Q \underset{k_{14}}{\overset{k_{13}}{\rightleftharpoons}} E_f\text{–}Q \xrightarrow{k_{15}} E_f + Q$$

† This investigation was supported in part by Research Grant AI1106 from the National Institutes of Health (1979–1984) and in part by the Graduate School of the University of Wisconsin. D.B.N. is the recipient of Career Development Award GM00254 from the National Institutes of Health. A preliminary report has appeared (Gates & Northrop, 1986).

* Author to whom correspondence should be addressed.

‡ Present address: Department of Biochemistry, University of Wisconsin, Madison, WI 53706.

0006-2960/88/0427-3834$01.50/0

Because the kinetic method of employing alternative substrates is new, a means of corroborating this mechanism was sought. Competitive product inhibition by the first product is the standard method of corroboration, but this kinetic pattern cannot be determined because pyrophosphate is consumed in the coupled assay. Another method is a value of zero for the ratio of the sum of the vertical coordinates of the crossover points of initial velocity patterns for the forward and reverse reactions to the sums of the maximal velocities in both directions (Janson & Cleland, 1974). However, the presence of extreme substrate inhibition by the majority of aminoglycosides in the forward reaction of ANT(2'')-I precludes accurate evaluation of the crossover coordinate from an initial velocity pattern.

More recently, viscosity dependence has been used as an indicator of diffusion control in enzymatic and nonenzymatic reactions (Carapellucci, 1975; Cerjan & Barnett, 1972; Solc & Stockmayer, 1973). For example, Kirsch and co-workers determined the diffusion-controlled components of the reactions catalyzed by chymotrypsin, β-lactamase I, and acetylcholinesterase by examining the effect of viscosity (Brouwer & Kirsch, 1982; Hardy & Kirsch, 1984; Bazelyansky et al., 1986). In addition, viscosity dependence has been used to probe relative rates of internal segments of enzymatic catalysis. For example, the variation of isotope effects with viscosity allowed Grissom and Cleland (1985) to dissect the forward commitment to catalysis of the reaction catalyzed by NADP-dependent malic enzyme into its internal and external components. In a Theorell–Chance kinetic mechanism, catalytic turnover is expected to be limited by the diffusion of the second product away from the enzyme, and thus it should be sensitive to changes in the viscosity of the solution surrounding the enzyme. The results reported here satisfy this expectation and support the rate-limiting release of the AMP–aminoglycoside.

Enzyme activity as a function of pH has been reported for only a few of the aminoglycoside-modifying enzymes and then only in the presence of excess concentrations of substrates (Radika & Northrop, 1984; Santanam & Kayser, 1976; Williams & Northrop, 1976). Van Pelt and Northrop (1984) reported that the activity profile of ANT(2'')-I with tobramycin and ATP as substrates has a sharp peak with an unusually high optimum of pH 9.5. They postulated that the high optimum was reflective of tight binding of the AMP–aminoglycoside product and its subsequent slow release from the enzyme. They speculated that as the amino groups of the AMP–aminoglycoside become deprotonated at higher values of pH, the product is released more rapidly. Separation of the pH–activity profile of ANT(2'')-I into its kinetic components of V, V/K, and K_I of substrate inhibition is reported here, with similarities and differences that further corroborate the rate-limiting release of the AMP–aminoglycoside.

Experimental Procedures

Chemicals. The sulfate salts of gentamicin C_1, sisomicin, and netilmicin (*N*-ethylsisomicin) were the gifts of Dr. George Miller, Schering Corp. Adenosine triphosphate, NADP, UDP-glucose, glucose 1,6-bisphosphate, dithiothreitol, ethylenediaminetetraacetic acid (EDTA),[2] UDP-glucose pyrophosphorylase, phosphoglucomutase, glucose-6-phosphate dehydrogenase, glycerol, MES, MOPS, HEPES, TAPS, CHES and lysine were purchased from Sigma.

Kinetic Methods. Kinetic constants as a function of pH were determined according to the coupled enzyme assay described previously (Gates & Northrop, 1988a). The buffers used at each value of pH are identified in the figure legends, all at a concentration of 0.1 M. Linearity of the coupled assay with ANT(2'') concentration was confirmed at pH 6.0, 7.0, 8.0, 9.0, and 9.5. Saturating concentrations of ATP were used at each value of pH, and the ratio of Mg–ATP to unchelated ATP was maintained at 390:1. The total concentration of magnesium acetate necessary to give this ratio for any given nucleotide at the pH specified was determined by using the equations of Adolfsen and Moudrianakis (1978) and Morrison (1979) as described previously (Gates & Northrop, 1988a). The final assay volume was 1.0 mL, and 5-cm optical glass cuvettes were used.

Viscosity studies employed a stock solution of CHES buffer used in the standard assay which contained an appropriate amount of glycerol to give the desired increase in viscosity. The coupled enzyme assay was linear versus ANT(2'') concentration in all of the concentrations of glycerol used in kinetic measurements. The solution viscosity was estimated by linear interpolation of data from the *CRC Handbook of Chemistry and Physics* (Weast, 1979).

Ionization Constants of Sisomicin. Protonation of amino groups in amino sugars causes upfield chemical shifts in the ^{13}C NMR spectra of carbons in the β position relative to the methine bearing the amino moiety (Naito et al., 1980). Chemical shifts of the β-carbons of sisomicin as a function of pH were generously provided by Dr. T. L. Nagabhushan and Dr. P. D. L. Daniels, of Schering Corp.

Data Analysis. Kinetic data initially were fitted by nonlinear regression to eq 1 or 2, depending upon the presence

$$v = VA/(K + A) \quad (1)$$

$$v = VA/(K + A + A^2/K_I) \quad (2)$$

of substrate inhibition, and given constant weighting. Viscosity dependence of V and V/K data were fit to eq 3, which describes a linear function, after Loo and Erman (1977), and

$$Y = a + bX \quad (3)$$

[1] The concept of a rate-limiting step has been much abused and lacks an accepted definition (Northrop, 1981; Ray, 1983). Following Johnston (1966) and Boyd (1978), the concept as used here is restricted to reaction processes that are irreversible and first order. Because these processes may consist of several chemical steps, they are referred to as reaction segments. How rate limiting each segment is will be proportional to the amount of enzyme participating in it during steady-state turnovers at saturating concentrations of substrates—which provides both a definition and a method of identification. Despite the popularity of the convention of attempting to identify individual rate-limiting steps within a series of reversible steps, the concept cannot really be defended. For example, in Scheme III, if $k_{15} \ll k_{14}$ (which is very likely), then $V = k_{13}k_{15}/k_{14}$; hence the maximal velocity becomes directly proportional to the forward rate constants of two separate steps. An experiment that directly reduced k_{15} and caused a proportional decrease in V could (by this popular convention) properly be interpreted as identifying "the rate-limiting step" as the release of Q. But a different experiment that reduced k_{13} and caused an equally proportional decrease in V could then independently be interpreted as identifying a conformational change as "the rate-limiting step" also. But both cannot be truly rate limiting at the same time, and if changes in both steps are directly proportional to changes in rates, then "partially rate limiting" is an inaccurate designation as well. Moreover, such data tell us nothing about which so-called rate-limiting step is the slower of the two. In the present case, the release of Q could be orders of magnitude slower than the rate of the conformational change (i.e., $k_{15} \ll k_{13}$) and yet both steps would remain equally rate limiting by current convention, and that does not make sense.

[2] Abbreviations: EDTA, ethylenediaminetetraacetic acid; MES, 2-(*N*-morpholino)ethanesulfonic acid; MOPS, 3-(*N*-morpholino)propanesulfonic acid; HEPES, 4-(2-hydroxyethyl)-1-piperazineethanesulfonic acid; TAPS, 3-[[2-hydroxy-1,1-bis(hydroxymethyl)ethyl]amino]-1-propanesulfonic acid; CHES, 2-(cyclohexylamino)ethanesulfonic acid; IU, international unit(s).

Table I: Kinetic Constants of Aminoglycoside Substrates as a Function of Viscosity

substrate	viscosity (η_{rel})	V (IU/mg)	V/K (L mg^{-1} min^{-1})	K_I (μM)
sisomicin	1.0	9.68 ± 1.80	0.146 ± 0.014	154 ± 40.7
	1.7	3.35 ± 0.39	0.123 ± 0.017	214 ± 39.1
	2.6	2.49 ± 0.49	0.053 ± 0.008	193 ± 58.2
	3.7	1.45 ± 0.17	0.043 ± 0.005	183 ± 32.1
gentamicin C_1	1.0	6.15 ± 0.28	0.154 ± 0.012	1840 ± 352
	1.7	2.18 ± 0.079	0.119 ± 0.009	1680 ± 267
	2.6	1.28 ± 0.058	0.085 ± 0.007	1740 ± 365
	3.7	0.57 ± 0.024	0.058 ± 0.006	2633 ± 698
netilmicin	1.0	5.69 ± 1.20	0.00163 ± 0.00017	5120 ± 1530
	1.7	3.05 ± 0.45	0.00271 ± 0.00049	8500 ± 2380
	2.6	2.96 ± 0.63	0.00234 ± 0.00046	5900 ± 2160
	3.7	1.96 ± 0.25	0.00301 ± 0.00061	5150 ± 1210

weighted by values of standard errors. The viscosity data were also fit to eq 4 and 5 with constant weighting. The dependence

$$Y = a + b(1 + cX)/(1 + X) + dX(1 + cX)/(1 + X) + eX \quad (4)$$

$$Y = a + b(1 + X)/(1 + cX) + dX(1 + X)/(1 + cX) + eX \quad (5)$$

of V/K values on pH were fit to eq 6, which describes a

$$\log (V/K)_{app} = \log [(V/K)/[1 + H/K_a + (H/K_a)^2 + K_b/H + (K_b/H)^2]] \quad (6)$$

bell-shaped curve that has two dissociable groups with a single acidic pK and two dissociable groups with a single alkaline pK. Similarly, substrate inhibition constants were fit to eq 7 which also contains double acidic and alkaline ionizations.

$$(pK_I)_{app} = \log [K_I/[1 + H/K_a + (H/K_a)^2 + K_b/H + (K_b/H)^2]] \quad (7)$$

Maximal velocities were fit to eq 8, which is the equation for

$$\log V_{app} = \log [[V_l + V_h(K_a/H)]/(1 + K_a/H)] \quad (8)$$

WAVE (Cleland, 1982). Chemical shifts were fit to eq 9, the

$$\log CS_{app} = \log [CS/(1 + K_b/H)] \quad (9)$$

half-bell curve of an alkaline dissociation. All pH data were given constant weighting in the log form. In these equations, v is a measured velocity, V is a maximal velocity (with subscripts l and h indicating low and high pH, respectively), A is varied concentrations of antibiotic or nucleotide, K is a Michaelis–Menten constant, K_I is a substrate inhibition constant, K_a and K_b are ionization constants, X is relative viscosity, H is the hydrogen ion concentration, and CS is a chemical shift. All data were fit by using a Northstar Horizon computer and the BASIC nonlinear regression program of Duggleby (1984).

Results

Effects of Viscosity. The activity of ANT(2″)-I was measured as a function of varied concentrations of good substrates (sisomicin and gentamicin C_1) and a poor substrate (netilmicin, based upon V/K values), including concentrations high enough to cause substrate inhibition, in the presence of 20%, 30%, and 40% added glycerol to effect changes in viscosity. Table I lists the relative viscosities for the concentrations of glycerol employed and their effects on V, V/K, and K_I values. Maximal velocities decreased markedly with increasing viscosity for all three substrates. Notably, the magnitude of the decrease with sisomicin (6.7-fold) and gentamicin C_1 (10.8-fold) greatly exceeds the increase in viscosity (3.7-fold). Values of V/K decreased for sisomicin and gentamicin C_1 but increased somewhat with netilmicin. In contrast, the constants for substrate inhibition neither increased nor decreased for all three substrates as viscosity increased, although there were some random fluctuations in their measurement.

Because the effects of viscosity on reciprocals of rates for diffusion-controlled processes should be linear functions, the data of Table I were fit to eq 3, and the results shown in the reciprocal plots of Figure 1. Results with inhibition constants are not shown, as fits of all three sets of data had insignificant values of slopes. The plot for the effect of viscosity on $1/V$ for sisomicin, shown in panel A, intersects below the horizontal axis (intercept = −0.073 ± 0.063). Similarly, the effect on $1/V$ for gentamicin C_1, shown in panel C, also intersects below the horizontal axis (intercept = −0.89 ± 0.31), and the arrangement of the data points suggests an upward curvature. Both generate normal data for K/V that have positive slopes and intercepts, shown in panels B and D. In contrast, the effect on $1/V$ for netilmicin, shown in panel E, intersects above the horizontal axis (intercept = 0.17 ± 0.03), and the effect on K/V, shown in panel F, is clearly negative (slope = −116 ± 44).

Both the negative parameters and the upward curvature show that the data are inadequately described by a linear function. Instead, a function of viscosity raised to a higher power is required. Figure 2 shows the results of fits of the same data to eq 4 and 5. Because the equations have four parameters and each data set consists of just four points, parameters a, b, and e were confined to a value of zero, with the exception of a = 0.15 in panel E and b = 750 in panel F. Parameter c was confined to a value of 3 in all data sets after comparing the agreement between point and line from fits using larger and smaller values (see, for example, the dashed lines of panel F). Nonlinear regression which minimized the sum of squares as a function of the remaining parameter only gave values for d as follows: panel A, 0.070 ± 0.003; panel B, 13 ± 1; panel C, 0.16 ± 0.02; panel D, 9.3 ± 3; panel E, 0.036 ± 0.004; and panel F, 3.3 ± 32.

Effects of pH. The activity of ANT(2″)-I was measured as a function of varied concentrations of sisomicin, including concentrations high enough to cause substrate inhibition, at values of pH from 6 to 10. The pH profile of K_I for substrate inhibition by sisomicin is a bell-shaped curve shown in Figure 3 with pK values of 6.68 ± 0.08 and 8.22 ± 0.06, but with asymptotes having slopes greater than unity. The data fit to eq 7, which describes a curve with asymptotes of +2 and −2, representing two acidic and two alkaline ionizations, but did not fit well to the equation describing single acidic and basic ionizations, i.e., equation BELL of Cleland (1982). Thus, the profile requires at least four ionizable groups, two that are basic and that must be protonated and two that are acidic and

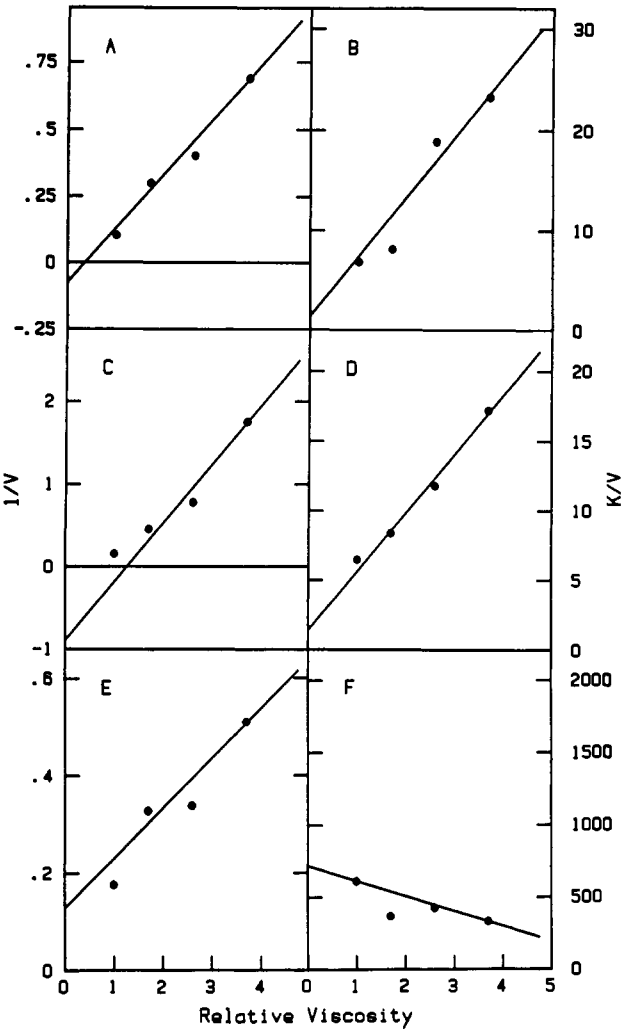

FIGURE 1: Reciprocals of V and V/K as a linear function of viscosity. Data from Table I on sisomicin are plotted in panels A and B, on gentamicin C_1 in panels C and D, and on netilmicin in panels E and F.

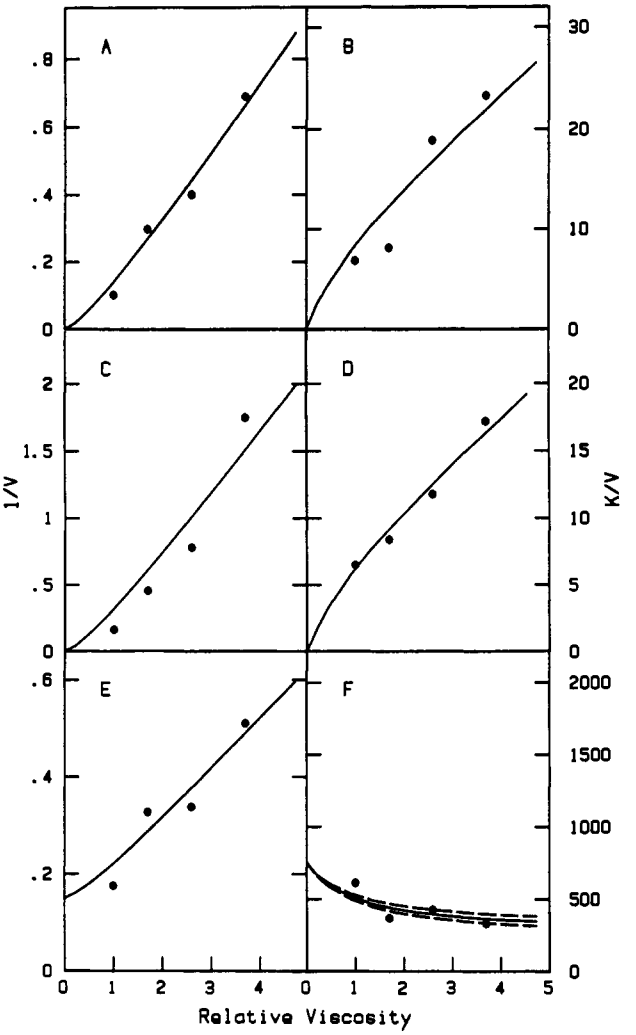

FIGURE 2: Reciprocals of V and V/K as a higher function of viscosity. Data from Table I on sisomicin are plotted in panels A and B, on gentamicin C_1 in panels C and D, and on netilmicin in panels E and F. Coefficient $c = 3$ for all solid lines and 2.5 and 3.4 for the dashed lines.

unprotonated, in order to express substrate inhibition. The pH profile of V/K values derived from variation of concentrations of sisomicin is shown in Figure 4. It is also bell shaped with pK values of 6.76 ± 0.07 and 8.45 ± 0.05. Like the pH profile for substrate inhibition, the data fit an equation describing a curve with asymptotes having slopes of +2 and −2. Thus, this profile, too, requires at least four ionizable groups, two protonated and two unprotonated, in order to express substrate activity. Moreover, the similar asymptotes and values of ionization constants for both V/K and K_I profiles strongly suggest a common origin.

The pH profile for maximal velocities with varied sisomicin is shown in Figure 5 and differs markedly from those obtained for V/K and K_I. This profile might appear to reflect a half-bell-shaped profile with decreasing activity at acidic pH, but when fitted to a straight line a slope of 0.32 was obtained, whereas half-bell profiles must have an asymptote with a slope of unity. Alternatively, the pH dependence of V can be adequately and more reasonably described by a shallow wave function. The solid line of Figure 5 was obtained by a fit of the data to eq 8, giving a pK of 8.4 ± 0.1 and values for V_l and V_h of 0.8 ± 0.1 and 11.1 ± 1.4, respectively.

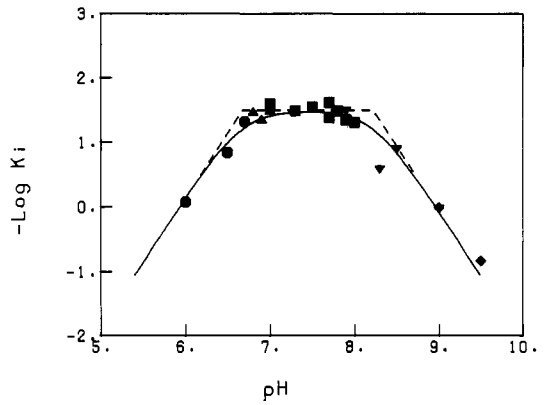

FIGURE 3: Profile of K_I of sisomicin as a function of pH. The dashed lines represent asymptotes with slopes of +2, 0, and −2, with breaks marking the ionization constants. The following buffers were used in this experiment: MES (●), pH 6.0, 6.5, and 6.7; MOPS (▲), pH 6.8, 6.9, and 7.0; HEPES (■), pH 7.0, 7.3, 7.5, 7.7, 7.8, 7.9, and 8.0; TAPS (▼), pH 7.8, 7.9, 8.0, 8.3, 8.5, and 9.0; and CHES (♦), pH 9.0, 9.5, and 10.0. The concentration of Mg–ATP was 8.23 mM for pH 6.0–7.9 and 14.13 mM for pH 8.0–10.0. The ratio of Mg–ATP to free ATP was fixed at 390.6:1 at all values of pH.

Discussion

Effects of Viscosity. The absence of any effect from increasing viscosity on the K_I values of substrate inhibition provides an important dual control. First, the lack of a consistent increase in K_I signifies that glycerol does not interfere with the binding of aminoglycosides to ANT(2'')-I. Second,

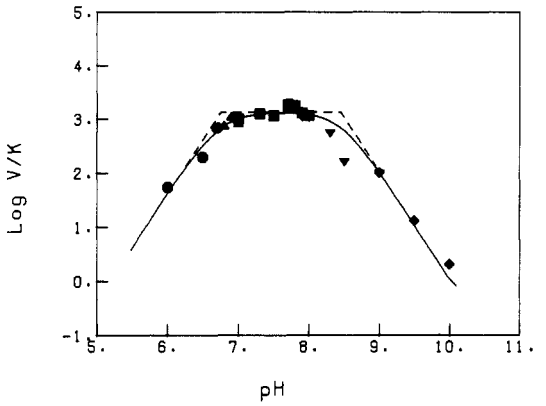

FIGURE 4: Profile of V/K of sisomicin as a function of pH. The dashed lines designate asymptotes with slopes of +2, 0, and −2, with breaks marking the positions of the ionization constants. The buffers and the Mg–ATP concentrations are described in the legend to Figure 3.

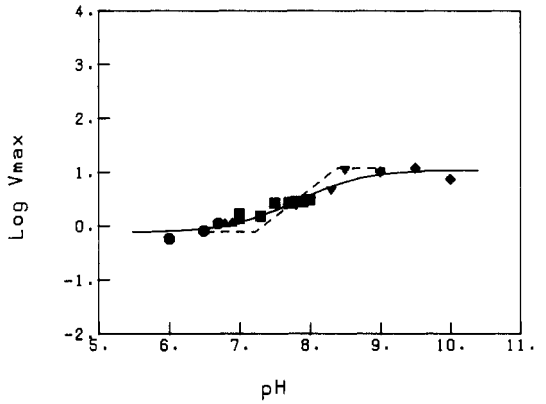

FIGURE 5: Profile of V of sisomicin as a function of pH. The dashed lines designate asymptotes of 0, 1, and 0, with the upper break marking the ionization constant. The buffers and Mg–ATP concentrations used are described in the legend to Figure 3.

the lack of a consistent decrease in K_I indicates that the steady-state distribution of E_c–Q of Scheme I (i.e., the form of enzyme to which aminoglycosides must bind to effect partial, uncompetitive substrate inhibition) does not increase despite changes of as much as 10-fold in maximal velocities. This finding is highly supportive of a Theorell–Chance kinetic mechanism.

The lack of a decrease in values of V/K for netilmicin is a second important control. It signifies that the productive binding of enzyme and netilmicin is not dependent upon a diffusion-controlled process, neither addition of substrate nor release of product. This was expected because netilmicin is the poorest aminoglycoside substrate of ANT(2″)-I, with a V/K more than 300-fold lower than that of sisomicin, for example (Gates & Northrop, 1988a); hence the conditions of rapid-equilibrium binding should obtain, independent of diffusion-controlled processes. Generally, a demonstration of such independence provides evidence that the viscosogen has no effect on catalysis, which is important to subsequent interpretation of data obtained with good substrates (Brouwer & Kirsch, 1982). In the present case, however, an unexpected increase is observed. However, steps other than those that are diffusion-controlled may be sensitive to changes in viscosity. For example, Kurz et al. (1987) have examined the effects of viscosity on slow-binding inhibitors of adenosine deaminase and detected a viscosity-dependent conformational change. Two conformational changes are proposed in Scheme I, one in the catalytic segment and one in the product-release segment. The former involves the conversion of E_fA to E_cA; the latter involves the opposite change in enzyme form, from E_c–Q to E_f–Q. Moreover, only the former can contribute to V/K in an ordered mechanism, whereas only the latter contributes to V in the proposed Theorell–Chance kinetic mechanism. Hence, if a change in viscosity altered the equilibrium between E_f and E_c, it would therefore express opposite changes on V and V/K as observed and would therefore be consistent with the Theorell–Chance kinetic mechanism outlined in Scheme I, in which an increase in viscosity favors the catalytic form of enzyme, E_c.

The kinetic expression for $1/V$ of Scheme I is given in eq 10, where the conformational changes and diffusion-controlled

$$\frac{1}{V} = \frac{1}{k_7} + \frac{1}{k_{11}} + \frac{k_{12}}{k_{11}k_{13}^\circ} + \frac{k_{12}k_{14}^\circ}{k_{11}k_{13}^\circ k_{15}^\circ} + \frac{k_8}{k_7k_9^\circ} \quad (10)$$

steps sensitive to viscosity are indicated as k°. If changes in viscosity affected the rates but not the equilibria of the conformational changes, i.e., if $k_{14}^\circ/k_{13}^\circ$ were constant, then eq 10 could be written in coefficient form as

$$\frac{1}{V} = a + b\eta_{rel} \quad (11)$$

where η_{rel} represents relative viscosity. Equation 11 predicts that the effects of viscosity on $1/V$ would still be a simple, linear function with a positive intercept, the same function as if only a single step were sensitive to the viscogen and in contradiction to the data in panels A and C of Figure 1. Thus, as has long been known with respect to isotope effects, multiple viscosity effects are not magnified in measured kinetic parameters.[3] Equations 10 and 11 show that the same is true for viscosity effects. However, unlike isotope effects, a viscosogen need not have an equilibrium effect near unity on non-diffusion-controlled steps, i.e., $k_{14}^\circ k_{13}^\circ$ need not be constant as above. If changes in viscosity did affect the equilibrium between forms of enzyme, with limits of $K_{eq} = [E_f]/[E_c]$ at zero and cK_{eq} at infinite viscosity, then the coefficient form of eq 10 becomes

$$\frac{1}{V} = a + \frac{b(1 + c\eta_{rel})}{1 + \eta_{rel}} + \frac{d\eta_{rel}(1 + c\eta_{rel})}{1 + \eta_{rel}} + e\eta_{rel} \quad (12)$$

With $c > 1$, eq 12 describes a hyperbola with upward curvature, approaching an asymptote with a positive slope of $e + dc$ and an intercept of $(a + b) - (bc + c)$, which could be either positive or negative. If the catalytic segment were rate-limiting, then eq 10 simplifies to

$$\frac{1}{V} = \frac{1}{k_7} + \frac{k_8}{k_7k_9^\circ} \quad (13)$$

which as a function of viscosity in coefficient form is the same as eq 11. On the other hand, if the product-release segment were rate-limiting, then eq 10 simplifies to

$$\frac{1}{V} = \frac{1}{k_{11}} + \frac{k_{12}}{k_{11}k_{13}^\circ} + \frac{k_{12}k_{14}^\circ}{k_{11}k_{13}^\circ k_{15}^\circ} \quad (14)$$

which as a function of viscosity in coefficient form is

$$\frac{1}{V} = a + \frac{b(1 + c\eta_{rel})}{1 + \eta_{rel}} + \frac{d\eta_{rel}(1 + c\eta_{rel})}{1 + \eta_{rel}} \quad (15)$$

Equation 15 retains the hyperbolic curvature and approaches an asymptote with a positive slope of dc and an intercept of $(a + b) - (bc + c)$.

[3] For example, two isotopically sensitive steps of an enzymatic reaction with effects of about 7 on each do not cause a change in the maximal velocity of either 14 or 49, but rather always express an overall isotope effect of 7 or less.

With four parameters describing a single line, the function is too complex and insensitive to converge in nonlinear regression, but confining all coefficients except d produced the regression lines that approximate the data in panels A and C of Figure 2; these are the same data that generated negative intercepts in Figure 1. Because negative values are not possible, the lines in Figure 2 provide better descriptions of the data.[4] Consequently, because their difference is dependent upon changing the forward rate constant of a step more than its reverse rate constant, these data require the presence of a non-diffusion-controlled step that is sensitive to the added glycerol and thus support the inclusion of the second kinetically significant conformational change in the mechanism of Scheme I.

Similarly, the kinetic expression for K/V of the second substrate of Scheme I is

$$\frac{K_b}{V} = \frac{(k_3^\circ + k_4^\circ)}{k_3^\circ}\left(\frac{k_6^\circ}{k_5^\circ k_7} + \frac{k_6^\circ k_8}{k_5^\circ k_7 k_9^\circ} + \frac{1}{k_5^\circ}\right) \quad (16)$$

Again, if changes in viscosity affect rates but not equilibria, eq 16 also reduces to the linear form similar to eq 11. But if the equilibrium between E_fA and E_cA were shifted to the right by the viscogen, then the coefficient form of eq 14 becomes

$$\frac{K_b}{V} = \frac{b(1 + \eta_{rel})}{1 + c\eta_{rel}} + \frac{d\eta_{rel}(1 + \eta_{rel})}{1 + c\eta_{rel}} + e\eta_{rel} \quad (17)$$

This kinetic function is also hyperbolic and similar to eq 12, but the position of coefficient c has changed. The curve has an asymptote with a slope of $e + d/c$ and an intercept of $b/c + 1/c$. With $c > 1$ and $d > b$, it curves downward, as shown in panels B and D of Figure 2. These lines were generated by setting coefficients b and e to zero in order to generate the maximum curvature. The data of panels B and D appear equally well described by the lines of either Figure 1 or Figure 2, so their comparisons tells us nothing about the significance or limits on the rate constants contributing to the coefficients of eq 17 and thus to V/K. But the linear description of Figure 1 requires dominance by coefficient e, representative of $1/k_5^\circ$ of eq 16, in direct contradiction to the results of substrate specificity studies which indicate that aminoglycoside binding is under rapid-equilibrium conditions (Gates & Northrop, 1988a). Instead, coefficient e must be absent, thus requiring $d > b$ in order to generate an asymptote with a positive slope, which in turn means that k_7 must be significantly greater than k_9 of eq 16; hence the data are correctly described by Figure 2, and the diffusion-controlled step contributing to V/K of the second substrates is the release of magnesium–pyrophosphate.

With $c > 1$ but $d < b$, however, the inverse hyperbole shown in panel F of Figure 2 is generated, which reflects an *increasing* V/K. Assuming that an increase in viscosity can only slow the rates of individual steps of an enzymatic turnover, these data require that a viscosity-sensitive equilibrium comes prior to the binding of the varied substrate. Because V/K represents the effective rate constant for combination with enzyme by substrate at very low concentrations, a reversible step preceding that combination must be at equilibrium, and the apparent V/K is dependent upon the amount of enzyme participating in that equilibrium that is in the form capable of combination. Therefore, even if increasing viscosity slows the rate constants k_3 and k_4 in Scheme I, by slowing k_4 more than k_3 it can shift the steady-state distribution of enzyme from E_fA to E_cA and increase the apparent value of V/K. Because netilmicin is the poorest substrate and displays rapid-equilibrium binding, its change in V/K with viscosity is solely dependent upon this shift in equilibrium. The data of panel F therefore support the inclusion of the first conformational change in the mechanism of Scheme I and place the magnitude of a viscosity-dependent rightward shift in equilibrium between 2.4 and 3.5 (see legend to Figure 2).

[4] Use of eq 12 to fit the data in panel E is not compelling, however, because of its clearly positive intercept and standard errors.

Table II: Ionization Constants of Amino Groups of Sisomicin

group position	β-carbon position	K_a	group position	β-carbon position	K_a
6′	5′	9.8	3	2	7.9
2′	3′	8.4		4	8.8
	1′	8.9	3″	4″	8.8
1	6	7.8		2″	8.9
	2	7.9		7″	8.8

Effects of pH. In an ordered kinetic mechanism, V/K of the first substrate is dependent on the bimolecular rate constant for combination with enzyme and cannot reveal anything about catalysis; hence, it is the V/K of the second substrate that is significant to pH kinetics. In these pH studies, the substrate used was sisomicin, an aminoglycoside that also gives strong substrate inhibition. Normally, the pH profiles of inhibition constants are easy to understand, as most are obtained with competitive inhibitors and reflect simple binding equilibria with free enzyme. But the substrate inhibition by sisomicin does not arise from binding to free enzyme; rather, it is caused by binding to the enzyme–AMP–aminoglycoside complex, E_c–Q, during the ordered release of products (Gates & Northrop, 1988b). The substrate inhibition constants, therefore, are also dependent upon the amount of E_c–Q present during turnover. Changes in pH that change the distribution of E_c–Q will be expressed in the substrate inhibition constants. The pH-independent region of Figure 3 coincident with pH dependence of the maximal velocity of Figure 5 shows that the steady-state concentration of E_c–Q is not sensitive to changes in pH. Together with the constancy of substrate inhibition constants during changes in viscosity, these data argue that virtually all of the enzyme is present as E_c–Q during catalytic turnover at saturating concentrations of substrate. This means that the kinetic mechanism of the enzyme does not change as a result of a change in pH. Also, it indicates that the pH profile for substrate inhibition shown in Figure 3 reflects true ionization constants.

The similarity of the V/K profile, shown in Figure 4, to the K_I profile argues that it also expresses binding of sisomicin to the enzyme, meaning that catalysis is pH-independent and that sisomicin binds to E_c–Q and to E_cA in the same manner. The similarity of the two profiles also shows that sisomicin is not a "sticky" substrate, because pK values are displaced outward from their true values when the rate of catalysis exceeds the rate of release of substrates (Cleland, 1982).

Structure–activity relationships for ANT(2″)-I argue that amino groups are crucial for binding of the aminoglycoside to the enzyme (Gates & Northrop, 1988a). It follows that the ionization states of the amino groups should be reflected in the pH profiles of the kinetic constants. Table II lists the ionization constants for the amino groups of sisomicin. The pK values for groups at positions 2′, 3, and 3″ are very close to the alkaline pK of both profiles, and all are likely candidates for involvement in binding, but only two of them are implicated. In the first of three papers in this issue (Gates & Northrop, 1988a), the 2′-amino group was identified as contributing to binding, which leaves either the 3 or 3″ as unimportant. The protonated form of the group at position 6′ may

Scheme II

$$\begin{array}{ccc} E_c\text{–}Q & & B \\ \Big\downarrow\!\uparrow 2H^+ & & \Big\downarrow\!\uparrow 2H^+ \\ E_cQ^{2+} & \rightleftharpoons E_c\text{–}Q^{2+} + B^{2+} & \rightleftharpoons E_cB^{2+}\text{–}Q^{2+} \end{array}$$

also contribute to binding, as it was also implicated in the first paper, but its pK borders the outside range of the data. Protonation of the group at position 1 does not contribute to binding because its pK lies within the pH-independent region of Figures 3 and 5.

The two acidic pK values of Figures 3 and 4 are clearly lower than any of the pK values of sisomicin. It is therefore necessary to assign these to the enzyme. They fall within the range of either histidyl or carboxyl groups buried in a hydrophobic pocket of the active site. Like-charge repulsion between side-chain histidines and aminoglycoside is a possible interpretation of the data, but pairing of two negatively charged carboxyls with the two positively charged amino groups of aminoglycoside which would enhance binding is a more attractive hypothesis.

The maximal velocity clearly has a different pH profile than V/K or K_I. Waves such as that in Figure 5 result when protonation decreases but does not eliminate a process or activity and are more common to V than to V/K or K_I profiles (Cleland, 1982). The pK of the wave is similar to the pK values for the amino groups at positions 2′, 3, and 3″ of sisomicin, two of which have already been implicated in aminoglycoside binding, and much higher than the ionization constants for the primary amino or secondary phosphate group of AMP (i.e., 3.7 and 6.1, respectively), which allows the possibility that the group responsible might be located on the aminoglycoside portion of the second product whose ionization might change k_{11} or k_{12} or both, in Scheme I and eq 14.

But there are problems with this possibility. If the release of the aminoglycoside portion of the second product contributed significantly to the maximal velocity and were pH-dependent, then the distribution of E_c–Q would have to be sensitive to both pH and viscosity, in contradiction to the data discussed above. For example, Scheme II illustrates the competitive segment between the binding of free aminoglycoside (B) to generate a dead-end complex responsible for substrate inhibition, in opposition to rebinding of the aminoglycoside portion of the second product. If the protonation of two amino groups on aminoglycosides favored binding of B and tighter binding of Q simultaneously, then the effects of a change in pH would cancel out. Consequently, in order for the binding of free sisomicin to E_c–Q and to E_cA to have similar pH profiles (Figures 3 and 4), the availability of the aminoglycoside-binding site on E_c–Q must be pH-independent. To account for this, the aminoglycoside portion of Q must be released during or after catalytic nucleotidylation but prior to the release of pyrophosphate to ensure that the return of E_c–Q to E_cQ does not occur, as illustrated in Scheme III.

Scheme III

$$E_f \underset{k_2}{\overset{k_1A}{\rightleftharpoons}} E_fA \underset{k_4}{\overset{k_3}{\rightleftharpoons}} E_cA \underset{k_6}{\overset{k_5B}{\rightleftharpoons}} E_cAB \underset{k_8}{\overset{k_7}{\rightleftharpoons}} E_cPQ \underset{k_{10}}{\overset{k_9}{\rightleftharpoons}} E_cP\text{–}Q \xrightarrow{k_{11}} E_c\text{–}Q + P$$

$$E_c\text{–}Q \underset{k_{14}}{\overset{k_{13}}{\rightleftharpoons}} E_f\text{–}Q \xrightarrow{k_{15}} E_f + Q$$

Energetics of the Kinetic Mechanism. Combining the results of viscosity-dependent and pH-dependent kinetics presents a very restrictive view of the energetics of this enzymatic reaction, illustrated in Figure 6 as a qualitative free energy

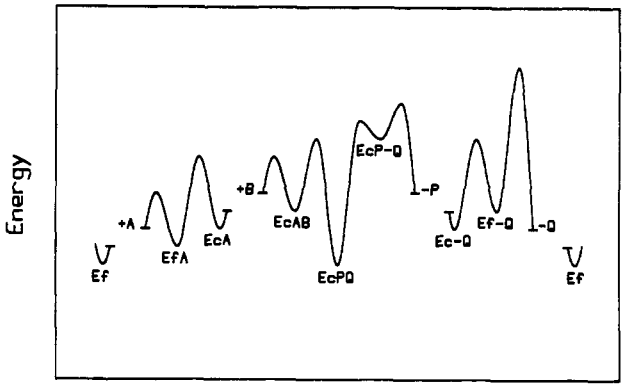

FIGURE 6: Free energy profile for an eight-step mechanism. The nomenclature is that described for Scheme I, and the sequences of steps derive from Scheme III.

diagram. The diagram consists of the eight steps shown in Scheme III and employs the nomenclature of Scheme I. To avoid problems of molecularity, portions of the reaction profile are separated by breaks in the curve, signifying the binding of substrate or release of product. These breaks divide the diagram into three significant parts. The first, following the binding of substrate A, shows the enzyme as two conformers with the energy level of E_fA lower than E_cA. The second begins with the binding of substrate B, continues with the catalytic nucleotidylation and the partial release of the aminoglycoside portion of AMP–antibiotic, Q, and ends with the release of magnesium–pyrophosphate, P. The latter would not be thought of immediately as a relatively "slow step" because of the small size, neutral change, and easy solvation of P; but setting a relatively "fast step" on top of an endothermic step nevertheless can make it a "most sensitive step" (Ray, 1983). The third portion of the diagram, ending in the release of Q which has the highest energy barrier of the diagram, again illustrates the two conformers of enzyme, but here the free form of enzyme is at a higher energy level than the catalytic form (i.e., E_f–Q > E_c–Q).

The conversion of the phosphate anhydride bond of ATP to an AMP–aminoglycoside ester is a highly exothermic process (i.e., approximately 4000 kcal) equivalent to a difference in energy level of 3 orders of magnitude. It is offset in Figure 6 by the partial release of the aminoglycoside which should be an endothermic process because the extended aminoglycoside poised above its binding site (i.e., E_cPQ, E_cP–Q) would be highly unstable. From an energetic point of view, these steps ought to be combined so that the first might drive the second. Moreover, combining these steps is favored by the stereochemical course of the reaction. Van Pelt et al. (1986) have shown that nucleotidylation catalyzed by ANT-(2″)-I proceeds with an inversion of configuration, consistent with an S_N2 displacement in which the incoming nucleophile displaces pyrophosphate in a single step through a trigonal-bipyramidal transition state. Such associative mechanisms are normally depicted with incoming and leaving groups in the apical position and with inversion expressed as movement of groups in equatorial and apical positions. But, as illustrated in Scheme IV (where Gen–OH represents the 2″-hydroxyl of gentamicin and Ado is adenosine held firmly in an equatorial position by the enzyme as indicated by the shaded area), it is the incoming nucleophile itself that must move during bond formation. Because the nucleophile is a secondary hydroxyl incorporated in a six-membered ring, its bonding to phosphate and thus its position relative to adenosine assumes a very rigid orientation (P. A. Frey, personal communication).[5]

Scheme IV

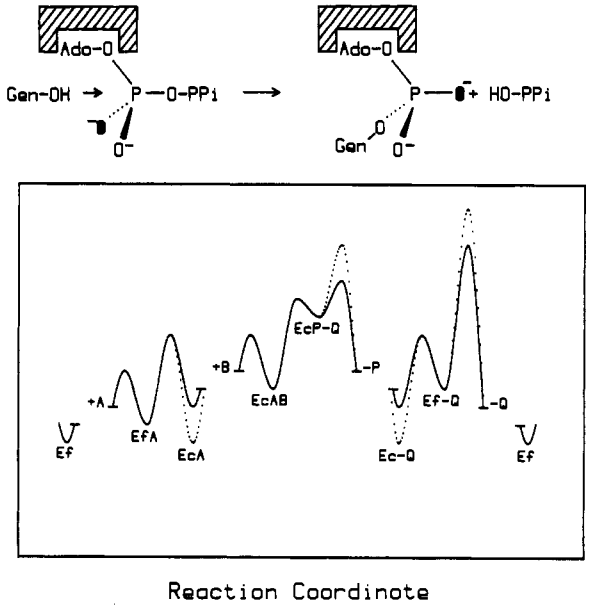

FIGURE 7: Free energy diagram for a seven-step reaction mechanism showing the effects of an increase in viscosity. The dotted line illustrates the changes derived from an increase in viscosity.

Figure 7 shows a second free energy diagram in which these two steps are combined. An advantage to catalytic turnover is immediately apparent, in that the low-energy "well" represented by E_cPQ of Figure 6, into which enzyme would otherwise accumulate, is avoided.[6] The solid line represents the energetics of the better substrates in an aqueous medium, whereas the dotted lines show the changes caused by an added viscosogen.[7] The first and third are effects on conformational equilibria as expressed by a suppression of the ground states of E_cA and E_c-Q only, but it is equally possible that the effects are expressed alternatively as an elevation of the ground states of E_fA and E_f–Q only. The second and fourth effects are on the diffusion-controlled release of products, P and Q, respectively. The combination of two effects of viscosity on the rate-limiting segment shown in the third portion of the diagram illustrates the origin of the marked and unusually large effects on maximal velocities; a decrease in the steady-state concentration of E_f–Q (e.g., 3-fold if equivalent to the change in E_fA; cf. panel F of Figure 2) coupled to an increase in the transition state for the release of Q (e.g., 3.7-fold if equivalent to the change in viscosity) creates a multiplier of effects (e.g., $3 \times 3.7 = 11.1$; cf. 10.8 for gentamicin C_1, Table I).

Conclusion. The results of the effects of changes in pH and viscosity identify eight individual steps in the reaction mechanism of ANT(2'')-I, place these steps in a specific order, and establish which are rate-limiting. Unprecedented in enzyme kinetics is the assignation of an ordered release of two products in which a portion of the second must be released prior to the release of the first. A practical implication of this finding is that inhibitors designed as multisubstrate analogues are not likely to be tight binding and thus not likely to block antibiotic resistance. Of a more general nature, the viscosity data demonstrate that this kinetic technique can be extended beyond an analysis of substrate binding and V/K to include assessments of the rate limitation of product release of V and to the detection of conformational changes.

ACKNOWLEDGMENTS

We thank Ronald G. Duggleby and Jack F. Kirsch for critical reading of the manuscript.

REFERENCES

Adolfsen, R., & Moudrianakis, E. N. (1978) *J. Biol. Chem. 253*, 4378–4379.
Bazelyansky, M., Robey, E., & Kirsch, J. F. (1986) *Biochemistry 25*, 125–130.
Boyd, R. K. (1978) *J. Chem. Educ. 55*, 84–89.
Brouwer, A. C., & Kirsch, J. F. (1982) *Biochemistry 21*, 1302–1307.
Carapellucci, P. A. (1975) *J. Phys. Chem. 79*, 2768–2773.
Cerjan, C., & Barnett, R. E. (1972) *J. Phys. Chem. 76*, 1192–1195.
Cleland, W. W. (1982) *Methods Enzymol. 87*, 390–405.
Duggleby, R. G. (1984) *Comput. Biol. Med.* 14, 447–455.
Gates, C. A., & Northrop, D. B. (1986) *Fed. Proc., Fed. Am. Soc. Exp. Biol. 45*, 1866.
Gates, C. A., & Northrop, D. B. (1988a) *Biochemistry* (first of three papers in this issue).
Gates, C. A., & Northrop, D. B. (1988b) *Biochemistry* (second of three papers in this issue).
Grissom, C. B., & Cleland, W. W. (1985) *Biochemistry 24*, 3356.
Hardy, L. W., & Kirsch, J. F. (1984) *Biochemistry 23*, 1275–1282.
Janson, C. A., & Cleland, W. W. (1974) *J. Biol. Chem. 249*, 2562–2566.
Jencks, W. P. (1975) *Adv. Enzymol. Relat. Areas Mol. Biol. 43*, 219–410.
Johnston, H. S. (1966) *Gas Phase Reaction Theory*, Chapter 16, Roland Press, New York.
Kuryz, L. C., Weitkamp, E., & Frieden, C. (1987) *Biochemistry 26*, 3027–3032.
Loo, S., & Erman, J. E. (1977) *Biochim. Biophys. Acta 481*, 279–282.
Morrison, J. F. (1979) *Methods Enzymol. 63*, 257–293.
Naito, T., Toda, S., Nakagawa, S., & Kawaguchi, H. (1980) in *Aminocyclitol Antibiotics* (Rinehart, K. L., Jr., & Suami, T., Eds.) pp 257–294, ACS Symposium Series 125, American Chemical Society, Washington, DC.

[5] The inability of the aminoglycoside portion of Q to bind normally in the active site of ANT(2'')-I provides an explanation for the surprisingly high value of K_{is} of product inhibition by AMP–tobramycin versus ATP described in the second of three papers in this issue (Gates & Northrop, 1988b). Because of an entropic effect, the nucleotidylated aminoglycoside would be expected to bind much more tightly than either a free nucleotide or free aminoglycoside, but just the opposite result was observed. Considering the fact that multisubstrate analogue inhibitors sometimes bind so tightly that they cannot be removed even by gel filtration (Jencks, 1975), the unavailability of the aminoglycoside binding site to the final product is a probably necessary mechanistic consideration in order to attain a reasonable rate of turnover which is nonetheless limited by product release.

[6] Added in proof: One way of grasping the energetics of this mechanism is to consider it a reverse of the commonly held precept of enzymology, that some of the substrate binding energy is used to drive catalysis (J. Van Pelt, personal communication). This insightful observation in fact gives credence to the precept. Obtaining direct evidence that a substrate undergoes strain upon binding and that such strain accelerates catalysis has proven to be very difficult. The precept has been supported instead by indirect inference and observation, such as tighter binding of putative transition-state analogue inhibitors. In contrast, that some of the catalytic energy is used to accelerate the release of a sticky product is directly supported by the kinetic data on ANT(2'')-I. It follows that, in the reverse reaction, the converse of these energetics must conform to the common precept; specifically, in order for the nucleotide and antibiotic portions of AMP–aminoglycoside to occupy their respective binding sites, the phosphoester bond connecting them would have to be broken.

[7] Not shown in Figure 7 are likely effects on the diffusion-controlled rates of binding and release of substrates because these were not detected in the present experiments.

Northrop, D. B. (1981) *Biochemistry 20*, 4056–4061.
Radika, K., & Northrop, D. B. (1984) *Arch. Biochem. Biophys. 233*, 272–285.
Ray, W. J., Jr. (1983) *Biochemistry 22*, 4625–4637.
Santanam, P., & Kayser, F. H. (1976) *J. Infect. Dis. 134*, S33–S39.
Solc, K., & Stockmayer, W. H. (1973) *Int. J. Chem. Kinet. 5*, 733–752.
Van Pelt, J. E., & Northrop, D. B. (1984) *Arch. Biochem. Biophys. 230*, 250–263.
Van Pelt, J. E., Iyengar, R., & Frey, P. A. (1986) *J. Biol. Chem. 261*, 15995–15999.
Weast, R. C., Ed. (1979) *CRC Handbook of Chemistry and Physics*, pp D239–D240, CRC Press, Inc., Boca Raton, FL.
Williams, J. W., & Northrop, D. B. (1976) *Biochemistry 15*, 125–131.

Interaction of tRNAs and of Phosphorothioate-Substituted Nucleic Acids with an Organomercurial. Probing the Chemical Environment of Thiolated Residues by Affinity Electrophoresis†

Gabor L. Igloi
Institut für Biologie III, Universität Freiburg, Schänzlestrasse 1, D-7800 Freiburg, FRG
Received September 23, 1987; Revised Manuscript Received December 9, 1987

ABSTRACT: The interactions of 4-thiouridine and 5-[(methylamino)methyl]-2-thiouridine in tRNA and of phosphorothioate esters in nucleic acids with an organomercurial have been investigated. For this purpose, an affinity electrophoretic system has been developed in which the mercury derivative has been covalently immobilized in a standard polyacrylamide gel. The retardation of thiolated macromolecules was found to be sensitive to the chemical environment of the sulfur atom, giving characteristic interaction constants dependent on the nature of the modification and its accessibility to binding. The interaction could, in the case of tRNA, be abolished by conventional specific chemical modification of the thiolated bases, as well as by irradiation with ^{32}P-derived β-emission. Not only has the fractionation of sulfur-modified from unmodified species been attained but a quantitative application of the technique has made it possible to study the binding of mercury and, by competition, that of magnesium in terms of the conformation of tRNA.

Despite the emergence of HPLC systems suitable for the fractionation of macromolecules, electrophoretic methods have, in general, gained preference over chromatographic separations in many areas of molecular biology. However, when specific affinity interactions are considered, the use of electromotive force (electrophoresis) as an alternative to hydrodynamic pressure (chromatography) has, with the exception of immunoelectrophoresis, so far not been widely appreciated. Thus, although affinity electrophoresis has been the subject of a number of reviews (Hořejší, 1981, 1984), its application has been largely restricted to specific enzyme–substrate and glycoprotein–lectin investigations (Hořejší, 1981, and references cited therein).

We have recently demonstrated the utility of boronate-containing polyacrylamide electrophoresis gels as general affinity media for the fractionation of free *cis*-diol-containing nucleic acids (Igloi & Kössel, 1985, 1987). The relatively weak interaction of *cis*-diols with boronate derivatives was found not to be influenced by the chemical environment of the interacting functional group in nucleic acids, whether in terms of a ribose residue or in the case of the Q modification in tRNAs. However, one could expect that a functional group more sensitive to its electronic environment might reflect its altered reactivity by a modulation of its interaction with an appropriate ligand.

The strong interaction of sulfur-containing nucleic acids with organomercurials has been the subject of numerous reports [e.g., Scheit and Faerber (1973), Sunshine and Lippard (1974), and Maguire (1976)], while the use of mercurated column materials for the isolation of sulfur-containing macromolecules is well documented (Melvin et al., 1978; Sun & Allfrey, 1982; Zhang et al., 1984) and the matrices for such batch procedures are commercially available. The wide range of chemical environments available to the sulfur atom provides a range of compounds whose different reactivity toward mercury might be expected to permit high-resolution fractionation by affinity electrophoresis.

In order to test this possibility and to widen the scope of affinity electrophoretic application, the interaction of sulfur-containing nucleic acids, as exemplified by tRNAs containing s^4U[1] or mam^5s^2U and by phosphorothioate-substituted nucleic acids, with an organomercurial polyacrylamide gel during electrophoresis has been investigated.

Experimental Procedures

Synthesis of [(N-Acryloylamino)phenyl]mercuric Chloride (APM). Addition of 8 mL of acetonitrile to 0.35 g of (*p*-aminophenyl)mercuric acetate (Fluka) at 0 °C, followed by 2 mL of 1.2 M $NaHCO_3$, resulted in an almost biphasic suspension in which the solid remained as a white mobile pellet at the base of the reaction vessel. A total of 0.2 mL of acryloyl chloride (Fluka) was now added in 10-μL aliquots over a period of 10 min with vigorous stirring. A voluminous white

†This work was supported by a grant from the Deutsche Forschungsgemeinschaft (SFB 206) to Prof. H. Kössel.

[1] Abbreviations: s^4U, 4-thiouridine; mam^5s^2U, 5-[(methylamino)-methyl]-2-thiouridine; APM, [(*N*-acryloylamino)phenyl]mercuric chloride; APB, [(*N*-acryloylamino)phenyl]boronic acid; HPLC, high-performance liquid chromatography; TLC, thin-layer chromatography; Tris, tris(hydroxymethyl)aminomethane; Temed, *N,N,N',N'*-tetramethylethylenediamine; EDTA, ethylenediaminetetraacetic acid; DTT, dithiothreitol.

0006-2960/88/0427-3842$01.50/0